Journal of Geochemical Exploration 161 (2016) 98–111

Contents lists available at ScienceDirect

Journal of Geochemical Exploration

journal homepage: www.elsevier.com/locate/gexplo

Multivariate statistical analysis of the REE-mineralization of the Maw Zone, Athabasca Basin, Canada

Shishi Chen [a,*], Keiko Hattori [a], Eric C. Grunsky [b,1]

[a] Department of Earth and Environmental Sciences, University of Ottawa, 25 Templeton Street, Ottawa, Ontario, Canada
[b] Geological Survey of Canada, 601 Booth Street, Ottawa, Ontario, Canada

ARTICLE INFO

Article history:
Received 2 June 2015
Revised 13 October 2015
Accepted 18 November 2015
Available online 29 November 2015

Keywords:
Data analysis
Elemental assemblage
Multivariate methods
Mineralization prediction
Uranium deposits

ABSTRACT

To evaluate the relationship between the enrichment of rare earth elements (REEs) and U, we carried out a principal component analysis (PCA) of sandstones in the REE-rich Maw Zone in the Athabasca Basin, Canada. The Maw Zone, a breccia pipe with surface exposure of 300 × 200 m, consists of highly silicified, hematitized, tourmaline-rich rocks with high REEs (up to 8.1 wt.% as total REE oxides). It is ~4 km southwest from the south end of the Phoenix U deposits, however, rocks in the Maw Zone do not show high U (<7.8 ppm in most rocks). We used RQ-mode PCA to compute variable and object loadings simultaneously, which allows the displays of observations and the variables at the same scale. PCA biplots of the Maw Zone data show that U is strongly correlated with V, Cr, Fe, Ni, Cu, Na, Li and Ba, but very weakly correlated with heavy rare earth elements (HREEs) + Y, and inversely with light rare earth elements (LREEs) and P. Relative enrichment of HREEs, Y, and P suggests xenotime as the predominant host of the HREEs. The grouping of LREEs + Sr + Th + P suggests the probable occurrence of monazite and/or aluminum phosphate-sulfate (APS) minerals. A mineralogical study confirmed the common occurrence of xenotime and APS minerals. The positive association between U and Fe in the PCA plot in the Maw Zone suggests that U was transported by oxidized fluids. The absence of U mineralization in the Maw Zone is explained by low U in the oxidizing fluids, or a lack reducing fluids to precipitate U. The PC1 and PC2 may reflect the major element assemblages related to the REE mineralization. The comparison of the maps of PC scores and the concentrations of HREEs + Y and P shows that the scores of PCs are better indicating the hydrothermal REE mineralization. For prospecting HREEs, PC2 is more reliable than PC1 because PC2 has the largest variance of HREEs and the second largest variance of LREEs.

© 2015 Elsevier B.V. All rights reserved.

1. Introduction

1.1. Rare earth elements in Athabasca Basin

The Athabasca Basin is a large Paleo- to Mesoproterozoic sandstone basin that occupies much of the northernmost quarter of the province of Saskatchewan and a smaller portion of northeastern Alberta (Fig. 1). It is the most significant U producing district in the world. Although no rare earth elements (REEs) have been produced in the past or are currently being produced in the Athabasca Basin, most U deposits contain anomalously high concentrations of REEs (Normand, 2014). REEs are mostly hosted by allanite and phosphate minerals, such as monazite, cheralite and xenotime (Normand, 2014). The earliest record of the REE mineralization in the Athabasca Basin was provided by Union Oil Company of Canada Inc. for the "Wheeler River Yttrium Prospect" (Knox, 1985, cited in Normand, 2014), which was found by AGIP Canada Ltd. and renamed the "Maw Zone" (MacDougall, 1990; Quirt et al., 1991; Hanly, 2001). The total indicated and possible resources were estimated to be ca. 463,000 tonnes grading 0.21 wt.% Y_2O_3 equivalent (0.1 wt.% cutoff) (Knox, 1985 cited in Normand, 2014). Quirt et al. (1991) suggested that the Maw Zone is the shallow peripheral expression of U deposits that occur along the unconformity between sandstones and the basement.

1.2. Principal component analysis

Principal component analysis (PCA) is useful in describing multi-element associations of geochemical data that often reflect mineralogy. In this particular study, PCA may reveal the geological processes critical to REE mineralization or minerals hosting REEs. The objective of PCA is to reduce the dimensionality of a dataset with a large number of variables, while retaining as much as possible of the variation in the variables (Jolliffe, 1986). This reduction is carried out by transforming raw data to a set of artificial variables, principal components, which retain the variation of the original variables in decreasing order. PCA has been used in geoscientific studies to identify elemental assemblages

* Corresponding author.
E-mail address: schen162@uottawa.ca (S. Chen).
[1] Current address: Department of Earth and Environmental Sciences, University of Waterloo, 200 University Ave. W, Waterloo, Ontario, Canada.

http://dx.doi.org/10.1016/j.gexplo.2015.11.009
0375-6742/© 2015 Elsevier B.V. All rights reserved.

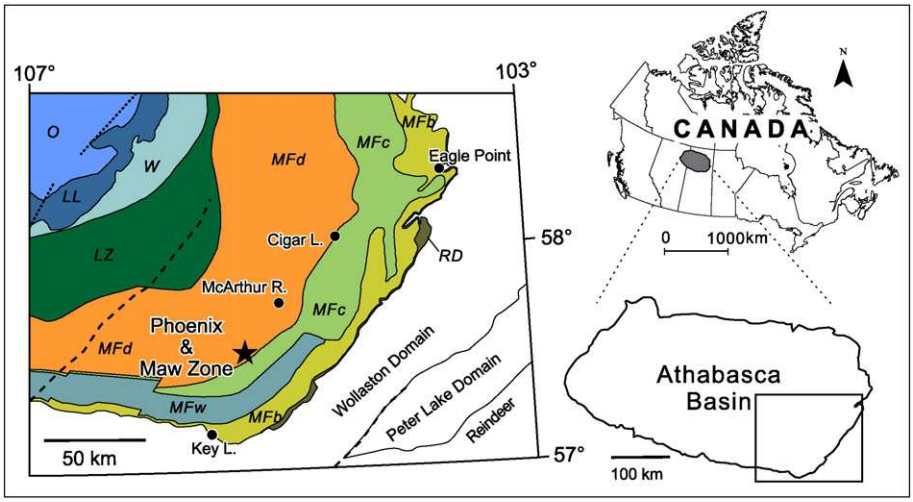

Fig. 1. General geological map of the southeast part of the Athabasca Basin, Saskatchewan, Canada (after Jefferson et al., 2007). Also shown is the position of the Phoenix U deposits and Maw Zone (solid star) and major unconformity-related uranium deposits (solid dots). RD = Read Formation; MF = Manitou Falls Formation (b = Bird Member; w = Warnes Member; c = Collins Member; d = Dunlop Member); LZ = Lazenby Lake Formation; W = Wolverine Point Formation; LL = Locker Lake Formation; O = Otherside Formation; The inserted map (upper right) shows the location of the Athabasca Basin within Canada. Boundaries of provinces are shown with thin black lines. The square in the lower right map shows the location of the main map within Athabasca Basin.

related to geological processes, such as hydrothermal alteration and mineralization (Grunsky, 1986).

1.3. The compositional nature of geochemical data

Geochemical data are reported as partial of a compositions (weight per cent, parts per million, etc.). Compositional data are unique in that the parts of a composition always sum to a constant (100%, 1,000,000 ppm). Thus for any D-part composition (x), D-1 parts are all that are required since the Dth composition is automatically defined as (constant $- \sum x_i) = x_D$. This problem was noted by Pearson (1897) and was largely ignored in the literature. Chayes (1960) attempted to deal with the problem using ratio correlations. Aitchison (1986) provided a solution to the problem by suggesting that the ratios are the most important information in any composition, and by taking the logarithms of the ratios, the values transformed range across the real number space, enabling the use of standard statistical methods to study geochemical data.

2. Study area

2.1. Geology

The Maw Zone is in the eastern part of the Athabasca Basin (Fig. 1) and ~4 km SW from the high-grade U ore of the Phoenix U deposits along the same NE-trending basement shear deformation zone (Fig. 2). AGIP Canada Ltd. (1985) discovered the enrichment in heavy REEs (HREEs) and Y in brecciated sandstones. The Maw Zone, with a surface exposure of 300 × 200 m, consists of highly silicified, hematitized, tourmaline-rich rocks with high REEs (up to 8.1 wt.% as total REE oxides; AGIP Canada Ltd., 1985). Tourmaline in the area has been described as dravite with varying Cr content (Quirt et al., 1991). The recent study of tourmaline chemistry in the Maw Zone suggests that it is magnesio-foitite (alkali-deficient Mg-rich tourmaline; O'Connell et al., 2015). Although the Maw Zone is close to the Phoenix U deposits, rocks do not show significantly high U (<7.8 ppm) except for one sample at a depth of 320 m in DDH WR195, which yielded 40.9 ppm U. The most prominent feature of the Maw zone is the intense hematitization and brecciation in sandstones. Some breccia fragments are large (up to 90 cm), and can retain primary sedimentary features, such as cross-bedding (MacDougall, 1990). The basement rocks in the area belong to the western Wollaston Domain of the Wollaston Supergroup that is Paleoproterozoic in age (Quirt et al., 1991; Yeo and Delaney, 2007; Jefferson et al., 2007). They are mostly graphite-, garnet- and cordierite-bearing, biotite metapelites, semipelites and quartzite and pegmatite lenses (Barker, 2011).

2.2. Sandstone stratigraphy

The eastern part of the Athabasca Basin is underlain by sandstones of the Manitou Falls Formation and the Read Formation. The Manitou Falls Formation is subdivided into three members in the area: the Dunlop Member, the Colins Member, and the Bird Member in stratigraphic order (Ramaekers et al., 2007, Table 1). The total thickness of sandstones in the Maw Zone varies greatly, from approximately 200 m in the western part to over 300 m in the eastern and northern parts of the Maw Zone. This large difference in the sandstone thickness is partly related to the paleo-topographic high of a quartzite "ridge" and the vertical movement along basement faults during the deposition of sandstones. The lowermost sandstone unit is lacking above the quartzite ridge. A major northeast-trending basement fault directly below the Maw Zone dips moderately to steeply to the east, occurring along a graphitic rock in quartzite and shows significant vertical displacement. Sandstones and quartzite close to the fault are brecciated, suggesting the ascent of hydrothermal fluids from the basement.

3. Samples

This study is based on chemical compositions of drill core sandstones (drill-hole locations are shown in Fig. 2) determined by the Saskatchewan Research Council for Denison Mines Corp. using an inductively coupled plasma optical emission spectrometer (ICP-OES) and mass spectrometry (ICP-MS) following the near total digestion using three acids (HF-HNO_3-HCl). Details of the analysis method and the quality assurance/quality control procedures are provided by Roscoe (2014).There is a total of 545 sandstone samples in the dataset. The elements in the original dataset include Al, Ag, Ba, Be, Ca, Cd, Ce, Co, Cr, Cu, Dy, Er, Eu, Fe, Ga, Gd, Hf, K, La, Li, Mg, Mo, Na, Nb, Nd, Ni, P, Pb, Pr, Sc, Sm, Sn, Sr, Ta, Tb, Th, Ti, U, V, W, Y, Yb and Zn. In this study, light REEs (LREEs) include La, Ce, Nd, Sm, and heavy REEs (HREEs), Gd, Dy, Er, and Yb. Europium is one of the LREEs, but it was not included in LREEs.

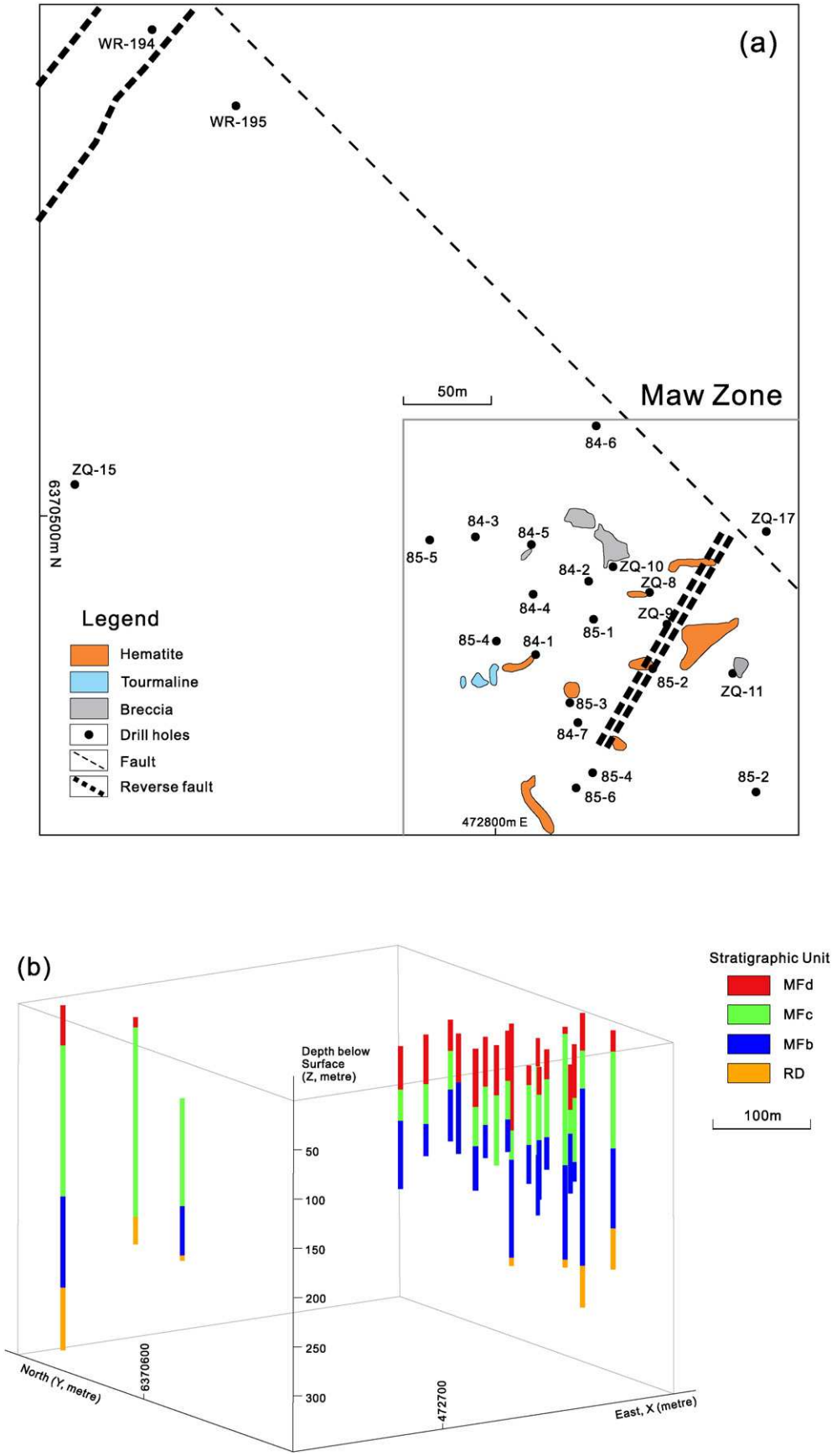

Fig. 2. (a): Drill hole locations and outcrops map. (modified after Pan, et al., 2013). Gray outline at lower right shows the REE mineralized Maw zone. The location of the faults are at the unconformity. WR-194 and -195 were drilled to target the edge of the quartzite ridge and provided samples with background values. ZQ-15 was drilled to evaluate anomalous concentrations of U and elements high in outcrops, including Ni, As, Co, Pb and B. No significant REE mineralization was found in these three drill holes. **(b)**: 3-D view map by Leapfrog™ program showing the occurrence of various stratigraphic units in the drill holes. Due to reactivation of basement faults, sandstone units are not horizontally continuous.

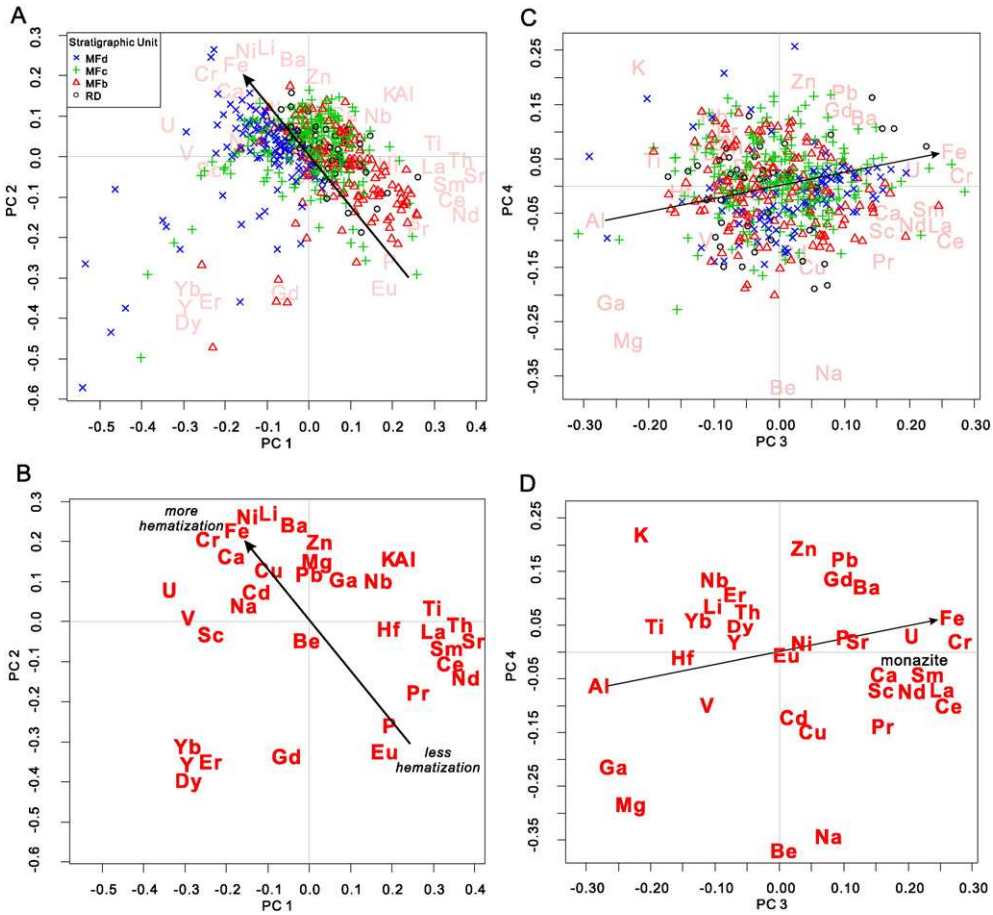

Fig. 3. Biplots of PC1 vs. PC2 and PC3 vs. PC4 for all sandstones data from the Maw Zone. Figures A and B, and C and D are identical, but B and D show only elements for the clarification. The data were transformed using a logcentred ratio. The R-loadings are scaled by a factor of 0.5 for better visualization of elements. In the biplot, samples with relatively high contents of a given element plot close to the position of the element and elements with coherent behavior plot in close proximity. The arrows show relative enrichment of Fe, reflecting the presence of Fe oxides in sandstones. Note the close association of U and Fe, and the separation of HREEs and LREEs in the diagram of PC1 vs. PC2.

4. Methodology

4.1. PCA

This study uses RQ mode PCA to process data. R mode (elements in this study) and Q (samples in this study) mode. RQ mode PCA allows the calculation of loadings (elements in this study) and object scores (samples in this study) simultaneously. This method was first described by Gabriel (1971) and termed "biplot". The biplot was further developed into RQ-mode PCA by Klovan and Imbrie (1971) and Zhou et al. (1983). Grunsky (2001) applied the method of Zhou in the R statistical environment. In this study, the elemental assemblages were evaluated using simultaneous RQ-mode PCA after a centered log-ratio transformation of the raw data (Aitchison, 1986) in order to overcome problems, caused by the "closed" nature of constant-sum compositional data. The statistical analysis was undertaken using the computing environment R (v. 3.1.0, R Core Team, 2013; Reimann et al., 2011).

The relative and actual contributions of the elements are calculated after PCA. The relative contribution is the contribution of a variable to all the components. For m variables (i = 1,....,m), p components (j = 1,...,p), ($p \le m$) and the R-mode loadings given by A^R, the relative contribution rc_{ij} for a variable j is given by the equation below (Grunsky, 2010):

$$rc_{ij} = 100 * \left[(A^R{}_{ij})^2 / \sum_{j=1}^{p} \left(A^R{}_{ij}\right)^2 \right]$$

The actual contribution is the contribution of a variable within a given component and defined as follows:

$$\mathrm{ac}_{ij} = 100 * [\left(\mathrm{A}^{\mathrm{R}}{}_{ij}\right)^2 / \sum_{j=1}^{m} \left(\mathrm{A}^{\mathrm{R}}{}_{ij}\right)^2)$$

4.2. Assessment of raw data before PCA

The elements Ag, Co, Mo, Sn, Ta, Tb and W show concentrations below, or close to, their detection limits, in >90% of the samples, and

Table 1
Stratigraphy of the Maw Zone.

Unit name		Number of samples	Lithology
Manitou Falls Formation	Dunlop Member (MFd)	113	Fine-grained quartz arenite with abundant (>1 vol.%) clay intraclasts
	Collins Member (MFc)	235	Quartz arenite with rare (<1 vol.%) clay intraclasts
	Bird Member (MFb)	155	Interbedded quartz arenite and conglomerate, distinguished from the underlying Read Formation and overlying MFc by the presence of conglomerate (>2 cm, 1–2 vol.%)
Read Formation (RD)		42	Poorly sorted quartz arenite and minor conglomerate

Table 2
Principal component analysis of Maw Zone sandstone data. Analysis is carried out on log centered transformed data.

2.1 Eigenvalues of PC1 to PC3.

Eigenvalue	PC1	PC2	PC3
λ	7.59	5.42	3.73
λ%	21.13%	15.08%	10.38%
Σλ%	21.13%	36.21%	46.59%

2.2 R-loadings of the elements

Elements	PC1	PC2	PC3	Sum of the square of the loadings PC1 to PC3
Al	0.45	0.32	−0.57	0.63
Ba	−0.08	0.49	0.26	0.31
Be	−0.02	−0.09	0.01	0.01
Ca	−0.38	0.33	0.33	0.36
Cd	−0.26	0.15	0.04	0.09
Ce	0.68	−0.20	0.52	0.78
Cr	−0.50	0.42	0.56	0.73
Cu	−0.20	0.26	0.10	0.12
Dy	−0.57	−0.75	−0.10	0.90
Er	−0.50	−0.71	−0.16	0.78
Eu	0.36	−0.64	0.02	0.54
Fe	−0.31	0.48	0.53	0.61
Ga	0.16	0.21	−0.52	0.34
Gd	−0.12	−0.67	0.21	0.50
Hf	0.38	−0.03	−0.30	0.24
K	0.43	0.31	−0.43	0.47
La	0.60	−0.07	0.48	0.59
Li	−0.21	0.55	−0.18	0.37
Mg	0.02	0.22	−0.47	0.27
Na	−0.32	0.09	0.15	0.13
Nb	0.33	0.21	−0.20	0.19
Nd	0.75	−0.24	0.41	0.78
Ni	−0.28	0.48	0.06	0.31
P	0.39	−0.51	0.20	0.45
Pb	−0.01	0.24	0.20	0.10
Pr	0.52	−0.35	0.32	0.49
Sc	−0.48	−0.06	0.31	0.33
Sm	0.67	−0.13	0.46	0.67
Sr	0.78	−0.06	0.24	0.66
Th	0.72	−0.01	−0.15	0.55
Ti	0.59	0.08	−0.39	0.51
U	−0.67	0.16	0.41	0.65
V	−0.58	0.02	−0.23	0.39
Y	−0.57	−0.71	−0.11	0.84
Yb	−0.55	−0.71	−0.24	0.86
Zn	0.04	0.40	0.07	0.17

2.3 Relative Contributions of elements to PC1

Relative contributions %			
Elements	PC1	PC2	PC3
Al	20.6	10.05	32.07
Ba	0.65	23.84	6.68
Be	0.04	0.79	0.01
Ca	14.4	11.05	10.93
Cd	6.82	2.33	0.16
Ce	46.73	3.83	27.51
Cr	24.56	17.38	31.11
Cu	4.08	6.89	1
Dy	32.47	56.79	1.09
Er	25.18	50.36	2.62
Eu	12.81	41.27	0.03
Fe	9.81	22.91	28.59
Ga	2.64	4.57	26.93
Gd	1.39	44.78	4.26
Hf	14.27	0.1	9.31
K	18.54	9.59	18.75
La	35.94	0.51	23.08
Li	4.23	29.89	3.4
Mg	0.03	5.02	21.77
Na	10.43	0.74	2.24
Nb	10.72	4.33	4.12
Nd	55.7	5.74	16.6
Ni	7.92	22.94	0.32
P	14.94	26.28	3.85
Pb	0.01	5.85	3.96

Table 2 (*continued*)

2.3 Relative Contributions of elements to PC1			
Relative contributions %			
Elements	PC1	PC2	PC3
Pr	27.1	12.31	10
Sc	23.32	0.35	9.64
Sm	44.61	1.66	20.75
Sr	60.18	0.42	5.72
Th	52.48	0.01	2.22
Ti	35.05	0.59	15.28
U	45.62	2.66	17.03
V	34.21	0.06	5.11
Y	32.92	50.36	1.25
Yb	29.99	50.56	5.8
Zn	0.18	16.2	0.53

2.4 Actual contributions of elements to PC1-3.			
Actual contributions %			
Elements	PC1	PC2	PC3
Al	2.71	1.85	8.58
Ba	0.09	4.39	1.79
Be	0.01	0.15	0
Ca	1.89	2.04	2.92
Cd	0.9	0.43	0.04
Ce	6.14	0.71	7.36
Cr	3.23	3.2	8.33
Cu	0.54	1.27	0.27
Dy	4.27	10.46	0.29
Er	3.31	9.27	0.7
Eu	1.68	7.6	0.01
Fe	1.29	4.22	7.65
Ga	0.35	0.84	7.21
Gd	0.18	8.25	1.14
Hf	1.88	0.02	2.49
K	2.44	1.77	5.02
La	4.73	0.09	6.18
Li	0.56	5.5	0.91
Mg	0	0.93	5.82
Na	1.37	0.14	0.6
Nb	1.41	0.8	1.1
Nd	7.32	1.06	4.44
Ni	1.04	4.23	0.09
P	1.96	4.84	1.03
Pb	0	1.08	1.06
Pr	3.56	2.27	2.68
Sc	3.07	0.06	2.58
Sm	5.87	0.31	5.55
Sr	7.91	0.08	1.53
Th	6.9	0	0.59
Ti	4.61	0.11	4.09
U	6	0.49	4.56
V	4.5	0.01	1.37
Y	4.33	9.27	0.33
Yb	3.94	9.31	1.55
Zn	0.02	2.98	0.14
ΣHREEs + Y	15.85	38.32	2.88
ΣLREEs	22.16	19.22	22.91

have been removed from the dataset. For the remaining elements, when concentrations are lower than the detection limit, they have been replaced by half the detection limit. In less than 5% of the samples, concentrations of some elements are not available and replacement values have been estimated using the "robCompositions" package (Templ et al., 2010) of the R program (R-Development Core Team, 2013). Since only small number (<1%) of values of important elements, such as Y, REEs, U, P and Fe, are missing in the dataset, we expect any potential bias related to imputed values is insignificant compared to the major geochemical patterns reported below. A training set with no censored values was used to estimate replacements for these censored values, based on a nearest -neighbor approach (Hron et al., 2010).

Aitchison (1986) suggested applying a log-ratio transform to the data to solve the "closure" problem caused by the nature of compositional data. Ratios are used because they do not change regardless of the effect of closure. A logarithm is applied to "open" the ratios into the real number space. This paper uses a centered log-ratio transformation of the data to obtain a symmetrical treatment of all parts of a composition as described by Aitchison (1986). The log-centered-ratio transformation changes from $\mathcal{S}^D$ to $\mathbb{R}^D$, where

$$\mathcal{S}^D = \left\{ x = (x_1, \ldots, x_D)', x_i > 0, \sum_{i=1}^{D} x_i = 1 \right\}$$

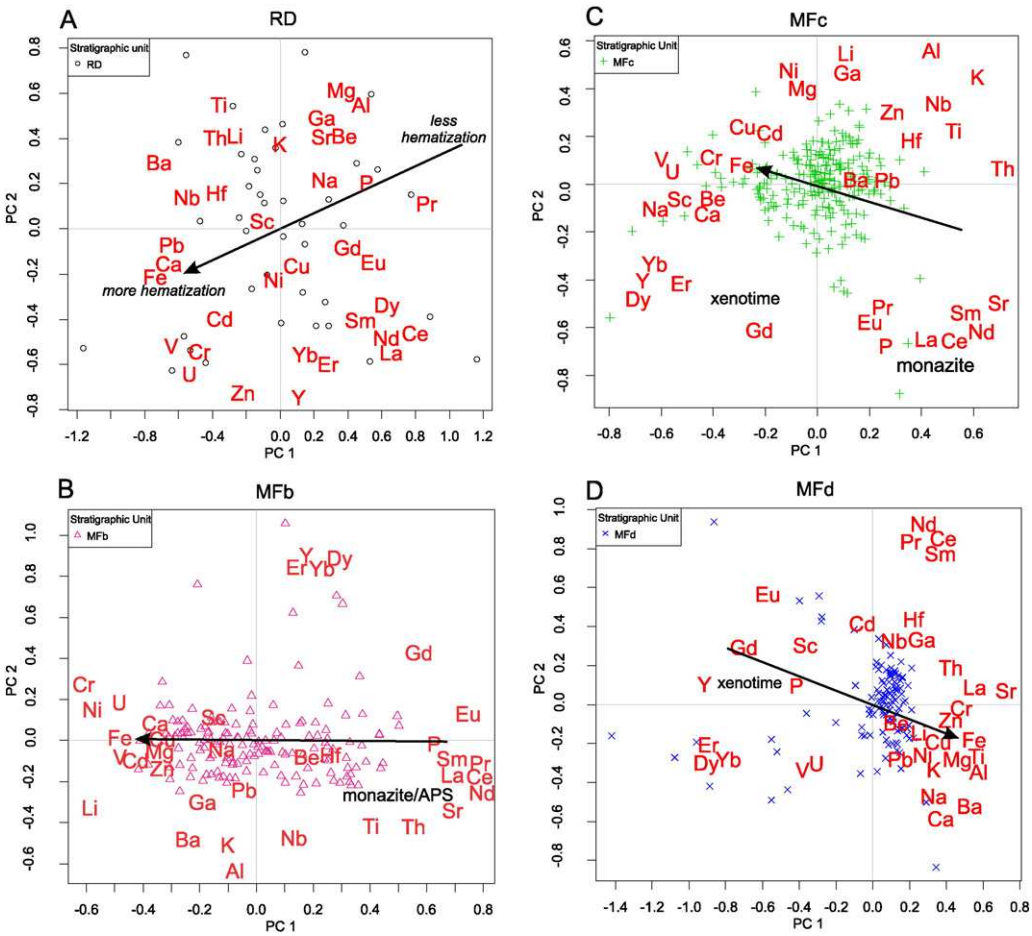

Fig. 4. Biplots of PC1 vs. PC2 for individual sandstone units from the Maw Zone. The data were transformed using logcentred ratio. The R-loadings are scaled by a factor of 0.5. The arrows show relative enrichment of Fe, reflecting the presence of hematite in sandstones.

Where the prime stands for transpose and the simplex sample space is a $D-1$ dimensional subset of $\mathbb{R}^D$.

And the result for an observation $\boldsymbol{x} \in \mathcal{S}^D$ is the transformed data $\boldsymbol{y} \in \mathbb{R}^D$ with

$$\boldsymbol{y}=(y_1,\ldots,y_D)' = \left(\log\frac{x_1}{\sqrt[D]{\prod_{i=1}^{D} x_i}},\ldots,\log\frac{x_D}{\sqrt[D]{\prod_{i=1}^{D} x_i}}\right)',$$

or written in matrix notation:

$$\mathrm{y} = \boldsymbol{F}\log(\boldsymbol{x}),$$

where.

$$\boldsymbol{F} = \boldsymbol{I}_D - \frac{1}{D}\boldsymbol{J}_D, \text{with}\,\boldsymbol{I}_D = \begin{pmatrix} 1 & & 0 \\ & \ddots & \\ 0 & & 1 \end{pmatrix}, \boldsymbol{J}_D = \begin{pmatrix} 1 & \ldots & 0 \\ \vdots & \ddots & \vdots \\ 0 & \ldots & 1 \end{pmatrix}$$

The matrices F, $\boldsymbol{I}_D$, and $\boldsymbol{J}_D$ have dimension D × D. The centered log-ratio transformation treats all components symmetrically by dividing by the geometric mean. Thus it is possible to use the original variable names for the interpretation of statistical results.

5. Results

5.1. PCA of the Maw zone dataset

R-mode loadings of elements, and the relative and actual contributions of the variables are shown for the first three components, which accounts for more than 46.6% of the variation in the data (Tables 2). The first two components account for 36.2%. The sums of the squares of the loadings for PCs 1 to 3 represent the proportion of the total variability for each element captured in the 3 PC model. The Sums of the squares of the loadings of REEs, Y and REEs in PC1-3 show high values, indicating that these three components capture the variability of those elements. The relative contributions of HREEs + Y in PC2 are 50.4% ~ 56.8% (largest among all PCs), and those in PC1 are 30.0%–32.5% (the second largest among all PCs). PC1, PC2 and PC3 contain most of the total variance of LREEs, which is reported 22.2%, 19.2% and 22.9% respectively.

The scores of PC1 and PC2 of all sandstone dataset are plotted in Fig. 3. Relative enrichment of HREEs and Y is observed along the negative PC2 axis in samples from the stratigraphic units MFb, MFc and MFd (Table 1) in PC1 vs. PC2 diagram (Fig 3A). HREEs are separated from LREEs, and the Eu is fractionated from the rest of REE (Fig. 3B). Iron plots in the upper left quadrant in Fig 3A. This indicates that the concentrations of Fe are relatively higher in rocks plotted towards the upper left quadrant.

PC3 and PC4 together account for 18.0% of the total variance. The biplot of PC3 vs. PC4 shows that the samples with relative enrichment in U, LREEs and P plot along the positive axis of PC3 (Fig. 3C and D).

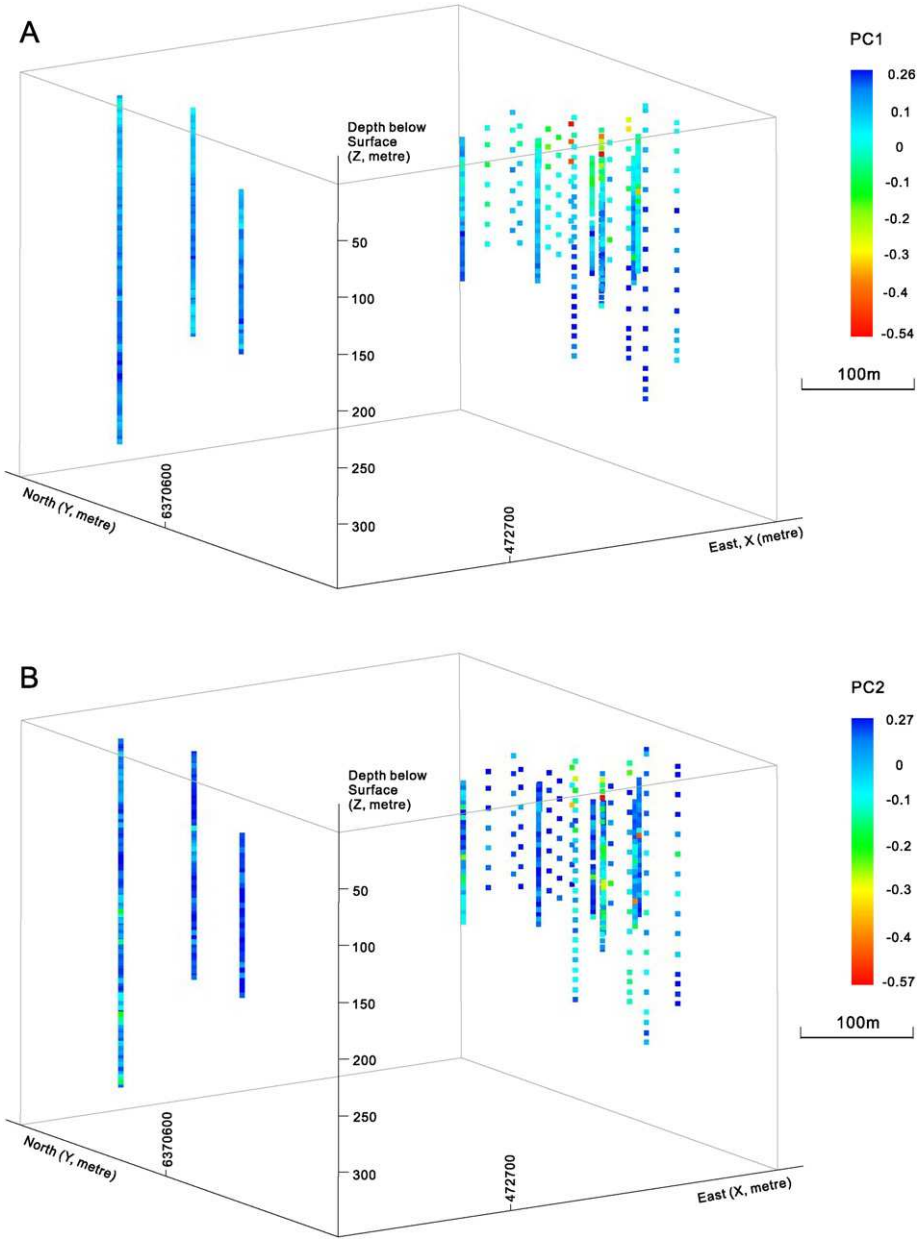

Fig. 5. Scores of PC1 (Fig. 5A) and PC2 (Fig. 5B) in drill holes in 3D space. The intervals of values in plotting are equal between the minimum and the maximum values.

PCA for individual sandstone units also has been carried out. In the PC1 vs. PC2 biplot for the RD data, U is associated with V and Cr and Fe. (Fig. 4A). The biplot for MFb shows the samples with relative enrichment in LREEs + P + Sr along the PC1 axis (Fig. 4B). The biplot of PC1 vs. PC2 for MFc shows that U is associated with Fe, Cr, V and Cu (Fig. 4C). Grouping of Sr-P + LREEs + HREEs + Y along the negative PC2 axis can be observed in Fig. 6C. The PC1 vs. PC2 biplot for MFd shows samples with relative enrichment in Y + REEs + P along the PC1 axis (Fig. 4D).

The scores of PC1 and PC2 of the total dataset in 3D space (Fig. 5) show negative scores of PC1 and PC2 mostly in the upper part of sandstones (MFc and MFd, Fig. 2b). This reflects that the REE mineralization in the Maw Zone is at shallow levels.

5.2. Mappings of PC scores and concentrations of HREE and P

Spatial distributions of PC scores and the concentrations of HREEs + Y and P are shown at different depths using Inverse Distance Weighting tool of ArcGIS 10.2.2. The distribution patterns for PC1 scores and the concentrations are similar at the surface (Fig. 6A), and the scores of PC1 show a smaller prospecting area on the map. This means that samples with high PC1 scores show high concentrations of HREEs and Y. The spatial distribution pattern of PC2 is very different from those of PC1 scores and concentrations. At 40 m depth map, the distribution pattern of PC2 and HREE show similar prospective areas, but the scores of PC1 provide a smaller area of high absolute values (Fig. 6B). Maps of PC1 scores and HREEs + Y contents at 100 m and 130 m depths show similar patterns (low absolute values of PC1 and HREEs, shown in Figs. 6C, D), but are very different from the map of PC2 scores. PC2 scores shows high absolute values due to high P contents at 100 m and 130 m depth.

5.3. Mineralogical studies

To evaluate interpretations based on the PCA, samples were collected from the areas of drill cores that show high scores of PC1 and PC2.

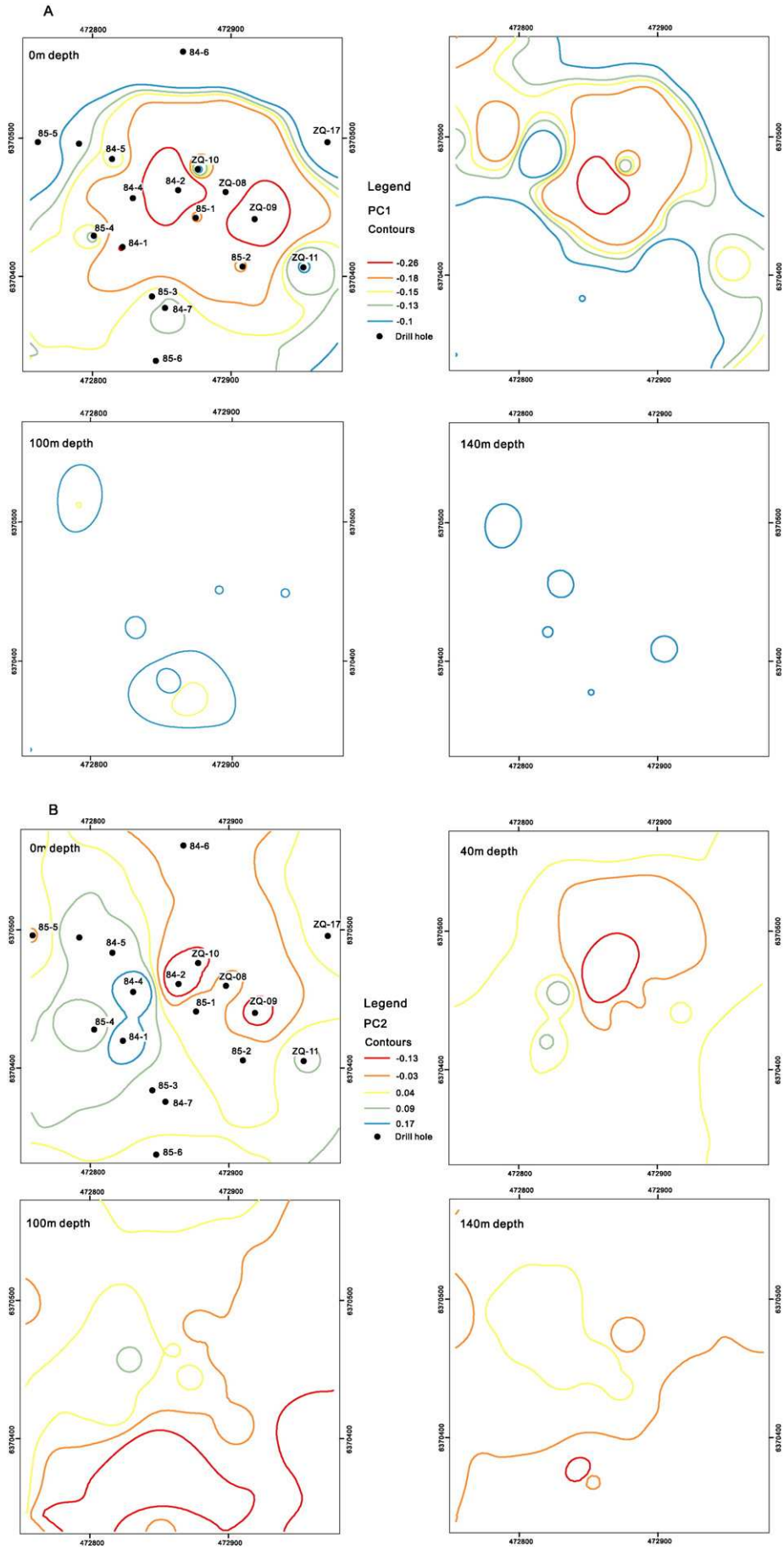
A
0m depth
100m depth
140m depth
Legend
PC1
Contours
-0.26
-0.18
-0.15
-0.13
-0.1
Drill hole
B
0m depth
40m depth
100m depth
140m depth
Legend
PC2
Contours
-0.13
-0.03
0.04
0.09
0.17
Drill hole
472800
472900
6370500
6370400
84-6
85-5
84-5
ZQ-17
ZQ-10
84-2
ZQ-08
84-4
85-1
ZQ-09
85-4
84-1
85-2
ZQ-11
85-3
84-7
85-6

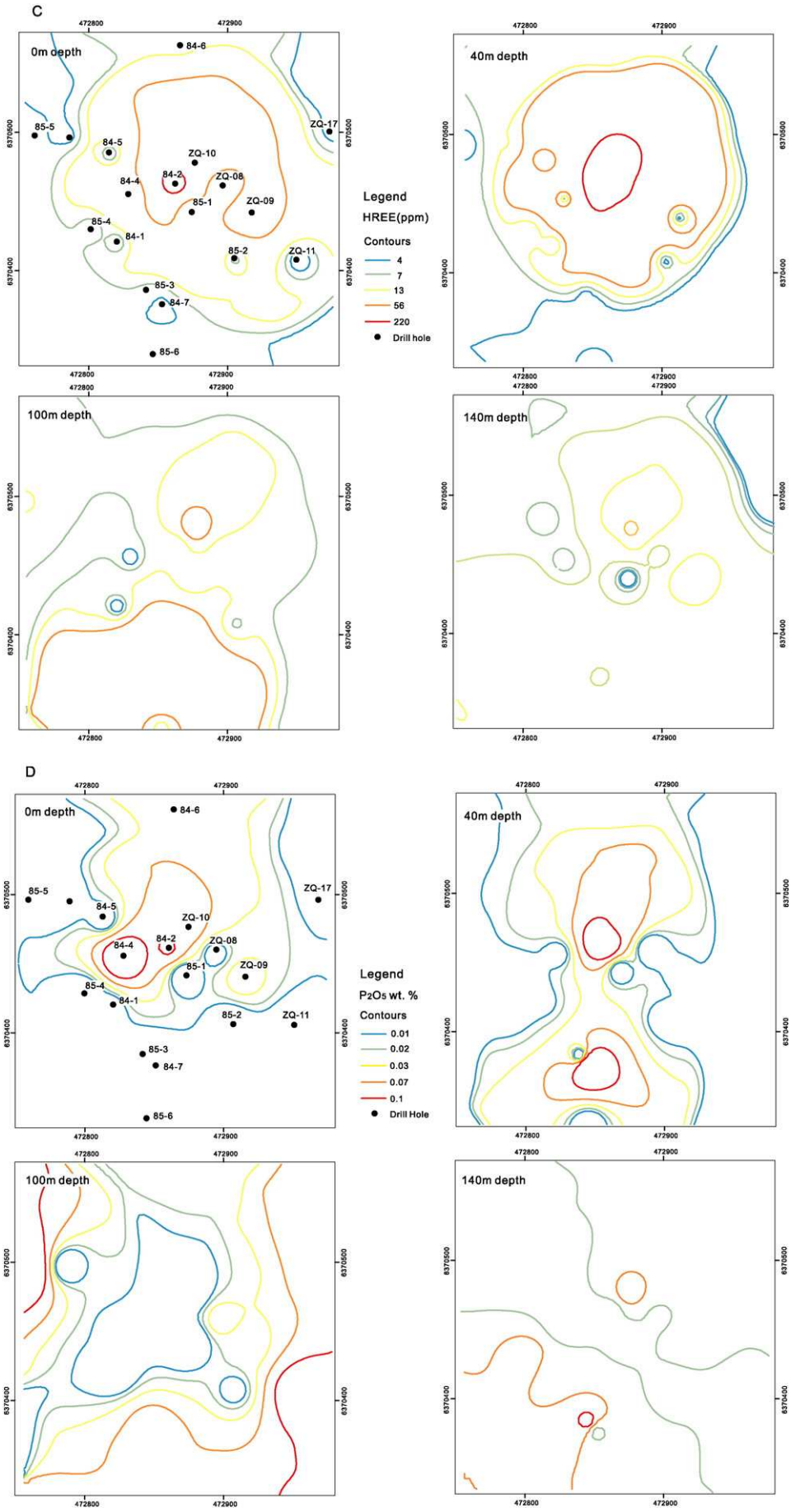
C
0m depth
40m depth
100m depth
140m depth
84-6
85-5
84-5
ZQ-17
ZQ-10
84-2
ZQ-08
84-4
85-1
ZQ-09
85-4
84-1
85-2
ZQ-11
85-3
84-7
85-6
Legend
HREE(ppm)
Contours
4
7
13
56
220
Drill hole
D
0m depth
40m depth
100m depth
140m depth
Legend
P2O5 wt. %
Contours
0.01
0.02
0.03
0.07
0.1
Drill Hole
472800
472900
6370500
6370400

Thirty-eight polished thin-sections were made from representative rock samples of all sandstone units and were examined using a petrographic microscope. They were also examined using a JEOL 6610 LV scanning electron microscope (SEM) equipped with an Oxford SDD detector after carbon coating of sections. Back scattered electron (BSE) images show the common occurrences of xenotime and other REE-bearing minerals. Xenotime shows two different styles of occurrence; the first style is subhedral to euhedral grains of xenotime that are spatially associated with detrital zircon grains (Fig. 7A, B, C, F, H). The second style is the dissemination of fine-grained xenotime in the groundmass of sudoite (Mg- Al-rich chlorite) without the presence of zircon grains (Fig. 7G). The fine-grained xenotime appears to have crystallized late from hydrothermal fluids. In addition, several small (<5 μm) grains containing high HREEs and Y occur around zircon crystals and show no P. The sum of HREEs and Y are over 50 wt.%. There are very few minerals that contain HREEs and Y greater than 50 wt.% without P. We therefore suggest that these grains are most likely Y-bastnäsite [(Y, HREE)CO_3F](Fig. 7D, E). The presence of F cannot be detected with SEM-EDS, but C counts were higher for the grains than the area outside the grains, suggesting that the grains contain carbon.

Aluminum phosphate-sulfate (APS) minerals are identified as the primary host of LREEs in our samples. APS minerals form veinlets and also occur as aggregates of small grains (Fig. 8A) in a matrix of aggregates of magnesio-foitite ± sudoite and illite (Fig. 8B). Semi-quantitative analysis of APS minerals with SEM-EDS suggests that they contain high Sr and LREEs. They also contain S and Ca, suggesting that the APS minerals are most likely solid solutions of svanbergite-florencite.

6. Discussion

6.1. Rare earth elements

Europium is separated from the rest of REEs in the biplot of PC1 vs. PC2 (Fig. 3A). Europium is commonly fractionated from the rest of the REEs because the valence of Eu is +2 and +3 in natural environments. Since Ca-rich plagioclase is the major host of Eu^{2+}, mafic igneous rocks commonly show positive Eu anomalies in chondrite-normalized REE patterns. On the other hand, felsic rocks commonly show negative Eu anomalies because of earlier removal of plagioclase. Moderate negative Eu anomalies occur in 95.9% of the sandstone samples, in the Maw Zone The median value of Eu anomalies ($[Eu/(\sqrt{Sm_N \times Gd_N})]$) is 0.45, suggesting contributions of REEs from felsic rocks. Considering that REEs were mostly introduced to the Maw Zone by hydrothermal activity, the evidence suggests interactions of the hydrothermal fluids with felsic rocks. It is not surprising considering that the rocks in the proximity are all felsic. The felsic component could be pegmatites and granitic orthogneiss abundant in the basement, and also pegmatite clasts in sandstones.

6.2. Elements associated with REEs

LREEs + P enrichment along PC1 and the position of P between HREEs and LREEs suggest that samples contain at least two phosphate phases (Fig.3B); one contains HREEs and another one contains LREEs. Their association with P suggests that HREEs and LREEs are likely hosted by xenotime and monazite, respectively.

The biplot of PC3 vs. PC4 of the total dataset shows that the samples with a relative enrichment in U, LREEs and P plot along the positive axis of PC3 (Fig. 3D), suggesting that LREEs are likely hosted by phosphate minerals, such as monazite or APS minerals.

An insight into elemental assemblages may be gained from the PCA results for the individual rock units. From the PC1-PC2 biplot for the RD data, U, Fe, V, Cr and REEs plot in the lower left quadrant, suggesting that the U- and REE-bearing minerals occur in oxidized sandstones. A weak association of P and REEs in RD suggests non-phosphorus minerals are likely contributing to REEs. The relative enrichment in LREEs + P + Sr along PC1 axis of the PC1 vs. PC2 biplot for MFb (Fig. 4B) indicates the possible occurrence of monazite and LREE-Sr-rich APS minerals. The elemental assemblage of Sr + P + LREEs + HREEs + Y along the negative PC2 axis of the PC1 vs. PC2 biplot for MFc (Fig. 4C) suggests the possible presence of APS minerals, monazite and xenotime. The relative enrichment in Y + HREEs + P along the PC1 axis of the PC1 vs. PC2 biplot for MFd (Fig. 4D), likely indicates the occurrence of xenotime.

6.3. Elements associated with U, Fe and Th

Uranium concentration is generally low and shows positive correlations with Fe, V and Cr (Fig. 3A). This suggests that small quantities of U precipitated under oxidized conditions. The enrichment of Fe is observed in the upper left quadrant in Fig 3A. Fe is most likely hosted by hematite, which is abundant in all rocks in the Maw Zone. Therefore, the enrichment of Fe is attributed to the presence of an oxidized environment. The PC1 and PC2 loadings for Fe show a distinct location in the upper left quadrant of Fig. 3A. This indicates that the concentrations of Fe are relatively higher in rocks plotted towards the upper left quadrant. Since rocks of MFd are mostly plotted in the upper left quadrant of PC1 vs. PC2 plot of the total dataset. The MFd unit appears to be more enriched in hematite compared to MFb and MFc. This is reasonable considering that the MFd is the farthest unit from the reduced basement rocks.

The association of Th + LREEs + P (Fig. 3B) suggests that the occurrence of APS minerals and/or monazite. APS minerals accommodate a variety of elements and those in sandstones are known to contain significant Th (Mwenifumbo and Bernius, 2007). Monazite is reported to contain significant Th at the Maw Zone, up to 3.5 wt.% ThO_2 (Pan et al., 2013)

6.4. Minerals containing REEs

Our mineralogical study identified xenotime, LREE-rich APS, and the probable occurrence of Y bastnäsite. Our results are consistent with the earlier report of the occurrence of xenotime by Quirt et al. (1991) and Hanly (2001). LREE-rich APS minerals are common in the Athabasca Basin, especially close to U ore (e.g., Adlakha and Hattori, 2015). APS minerals in our samples are svanbergite-florencite and they occur as the major host of LREEs. Monazite was not found in our samples, although it has been reported from the Maw Zone by Quirt et al. (1991),and Pan et al. (2013). The APS minerals in our samples show significant SO_4^{2-}, which confirms the oxidized environments for the hydrothermal activity.

6.5. Lack of uranium mineralization in the Maw zone

Quirt et al. (1991) suggested, based on similar alteration assemblages, that the REE mineralization in the Maw Zone is related to the uraniferous hydrothermal activity. Uranium concentrations in the Maw zone are overall low (<7.9 ppm in almost all samples), although the values are generally higher than the average crustal concentration of 0.91 ppm (Taylor and McLennan, 1985). The positive correlation between U and Fe and their loadings in the Fe-rich regions of the

Fig. 6. Maps showing the scores of PC1 and PC2, and HREE + Y and P concentration at 0 m, 100 m and 130 m depth. Small solid circles are the locations of drill holes. The isoline values are determined by 25th, 50th, 75th, 90th and 95th percentiles. Note that no significant REE mineralization was found in samples in drill holes WR-194, WR-195 and ZQ-15. These drill holes are far away from the mineralized area. Since there is no drill holes between these three holes and the mineralized area, the data of WR-194, WR-195 and ZQ-15 are removed from the dataset for minimizing the interpolation error of mapping.

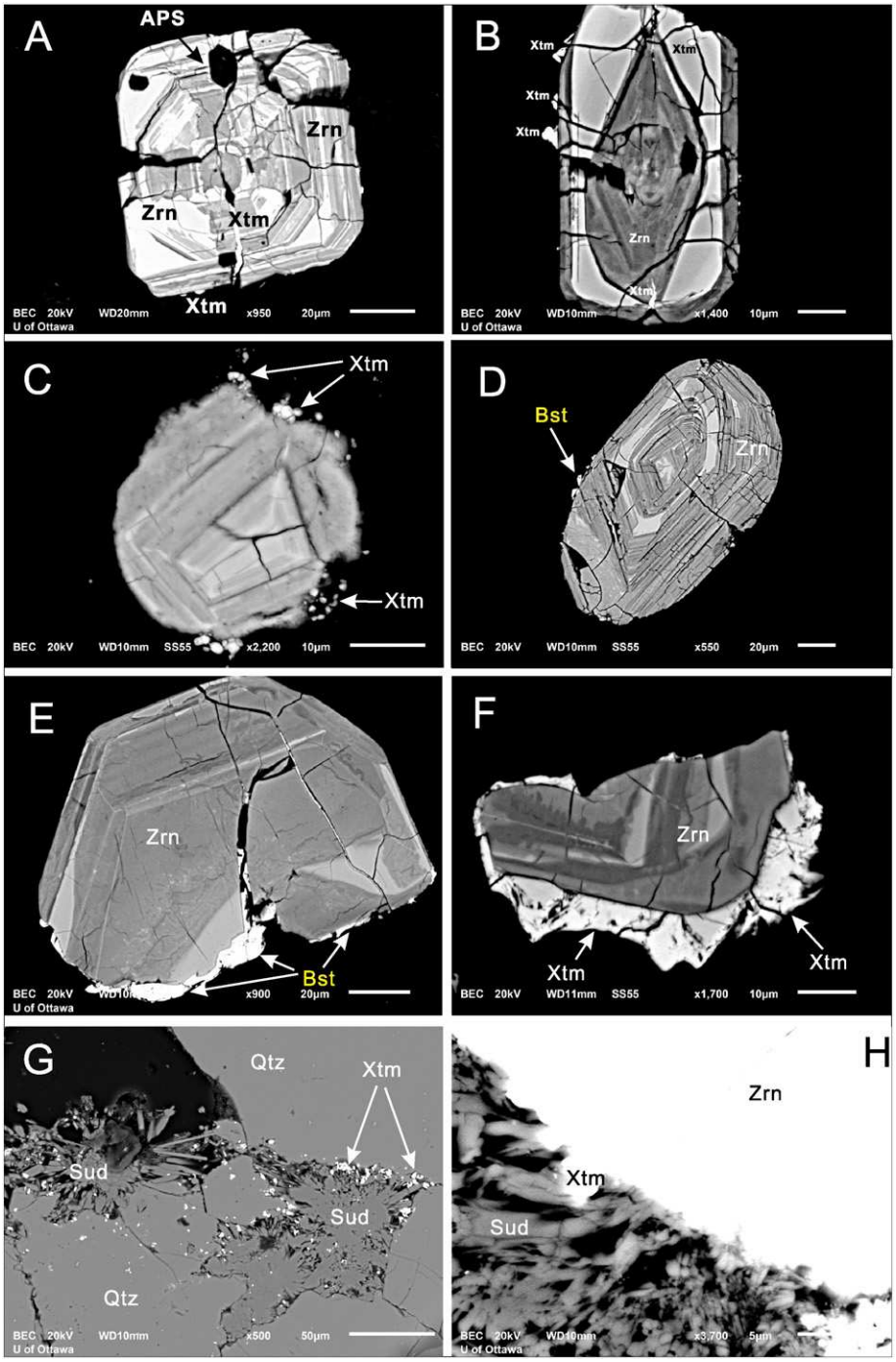

Fig. 7. BSE images of xenotime (Xtm) and bastnäsite (Bst) in sandstone samples from MFb (Fig. 7A: DDH 85-3, 102.5 m depth, Fig. 7B and H: ZQ-09, 215 m depth, Fig. 7G: DDH 85-3, 132.5 m depth), MFd (Fig. 7C: DDH 84-2, 30 m depth; Fig. 7D: DDH 84-2, 50 m depth), the RD (Fig. 7E: ZQ-09, 225 m depth, Fig. 7F: DDH WR-194, 357.5 m depth). Bst = bastnäsite, Mgf = magnesio-foitite, Qtz = quartz, Sud = Sudoite, Xtm = xenotime, Zrn = zircon

biplots (Fig. 3) suggests that U was transported by oxidized fluids and is associated with Fe oxides. Uranium may possibly be adsorbed on Fe-oxides/hydroxides and clays (Jefferson et al., 2007). Uranium is highly mobile in an oxidized solution where U forms soluble U^{6+}. The deposition of U requires reduction of U^{6+} to insoluble U^{4+} in a reducing environment (Jefferson et al., 2007).

There are two possible explanations for the absence of significant U mineralization in the Maw Zone. The concentrations of U in the oxidizing fluids were low, as suggested by Pan et al. (2013) based on the lack of radiation-induced defects in quartz. Alternatively, the oxidizing fluids did not encounter reducing fluids or media in the basement to precipitate U. Although REEs can be transported by acidic oxidizing brines similar to those which transport U (Fayek and Kyser, 1997; Adlakha and Hattori, 2015), no reducing conditions are required for the deposition of REE-bearing minerals.

6.6. Vertical variations of PCs and exploration in Maw zone

Since negative PC1 scores represent the enrichment of HREEs without P and negative PC2 scores represent both P REEs enrichment, the 3D

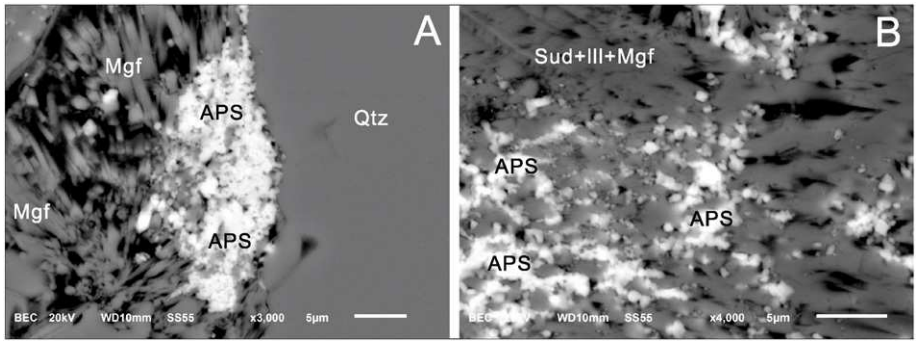

Fig. 8. BSE images of APS minerals (bright) in sandstone sample from MFd (DDH ZQ-08, 33 m depth). Ill = illite, Mgf = magnesio-foitite, alkali-deficient Mg-rich tourmaline, Qtz = quartz.

plotting of PC1 (Fig. 5A) clearly shows non-phosphorous HREEs enrichment at shallow depths (0–40 m) in the MFd and MFc units and plotting of PC2 (Fig. 5B) shows the enrichment of P + LREEs + HREEs at relatively deeper depths (40–150 m).

At the surface, the pattern of PC2 scores (Fig. 6B) is most likely influenced by LREEs and P, since negative PC2 scores also represent P and LREEs. At 40 m depth, PC1 map (Fig. 6A) shows smaller prospective areas than those of the PC2 (Fig. 6B) and HREEs + Y (Fig. 6C) maps. This may be due to HREEs + Y contents are decreasing but LREE contents increasing from 40 m depth. At 100 m and 130 m depths, PC1 values are not strong (Fig. 6A), therefore signature of HREE mineralization is weaker at these depths. However PC2 values (Fig. 6B) indicate strong LREE enrichments. High absolute PC2 values and high P contents are most likely caused by high contents of APS minerals hosting LREEs and P. The maps of P content for varied depth (Fig. 6D) show elevated values in the areas showing HREEs + Y enrichment, but P also can have high values in areas with no significant HREEs + Y enrichment. This is attributed to the presence of other P-bearing minerals, such as APS.

Although some samples show high HREEs + Y values at deep parts (depth below 100 m), the values are possibly caused by detrital minerals, such as zircon, which may contain HREEs. These high HREE contents are not related to hydrothermal mineralization and do not belong to the major multi-element association. Therefore, using PCs, which may represent major element assemblages corresponding to minerals that contain elements of interest, is helpful to reduce "noise" in the data and to assess areas with probable mineral resource than examining elements separately (as shown by Fig. 6C and D).

The data from drill holes at shallow depth (<100 m) shows high absolute PC1 values (HREEs + Y without P) but no significant PC1 values at deeper depth (>100 m), suggesting that deeper drilling is probably not necessary to get the mineralization of HREEs. PC1 has better discrimination for HREEs + Y and LREEs than PC2, therefore using PC1 is more suitable to observe possible non-phosphorus HREEs occurrence than PC2, although PC2 has larger variance of HREEs. In the case of prospecting both HREEs + P (xenotime) and LREEs + P (APS), PC2 provides a more favorable predictive map than PC1 in this area.

7. Summary

The application of RQ-mode PCA in the REE-rich Maw Zone shows elemental assemblages related to the mineralization. Xenotime is the main host of HREEs + Y, and APS minerals and/or monazite, for LREEs. The mineralogical study confirms that xenotime and bastnäsite are the main hosts of HREEs + Y and APS minerals for LREEs. There are two possible explanations for the lack of significant U mineralization in the Maw Zone: The concentrations of U in the oxidizing fluids were low. Alternatively, the uraniferous oxidizing fluids did not encounter reducing fluids that enabled the precipitation of U. Mapping the spatial distribution of scores of the significant PCs may be useful to provide more reliable estimates of the location of mineralization than using only single element mapping.

Acknowledgments

We thank Denison Mines Corp. for providing the geochemical data and approving the publication of this manuscript. We thank Chad Sorba and Yongxing Liu of Denison Mines Corp for their help in the field. We thank Glenn Poirier at the University of Ottawa for his help during the SEM study. We thank ARANZ Geo Limited for providing education license to use Leapfrog™ 3D geological modeling program. The research project is funded by a grant to KH from the Natural Resources of Canada through the TGI-4 uranium ore systems project. Comments from Julien Mercadier, Donald Wright and Eric Potter on the earlier draft were helpful. Comments from the anonymous reviewer greatly improved the manuscript.

References

Adlakha, E.E., Hattori, K., 2015. Compositional variation and timing of aluminum phosphate-sulfate minerals in the basement rocks along the P2 fault and in association with the McArthur River uranium deposit, Athabasca Basin, Saskatchewan, Canada. Am. Mineral. 100, 1386–1399.

Aitchison, J., 1986. The Statistical Analysis of Compositional Data. Chapman and Hall, London.

AGIP Canada Ltd., 1985. Assessment File 74H06-NW-0080. Sask (Energy and Mines. 113 pp.).

Barker, M., 2011. The Y and HREE Enrichment of the Maw Zone. Wheeler River preliminary Summary. Unpublished Report to Denison Mines. 16 pp.

Chayes, F., 1960. On correlation between variables of constant sum. J. Geophys. Res. 65, 4185–4193.

Fayek, M., Kyser, T.K., 1997. Characterization of multiple fluid-flow events and rare-earth-element mobility associated with formation of unconformity-type uranium deposits in the Athabasca Basin. Saskatchewan. Can. Mineral. 35, 627–658.

Gabriel, K.R., 1971. The biplot graphic display of matrices with application to principal component analysis. Biometrika 58, 453–467.

Grunsky, E.C., 1986. Recognition of alteration in volcanic rocks using statistical analysis of lithogeochemical data. J. Geochem. Explor. 25, 157–183.

Grunsky, E.C., 2001. A program for computing RQ-mode principal components analysis for S-plus and R. Comput. Geosci. 27, 229–235.

Grunsky, E.C., 2010. The interpretation of geochemical survey data. Geochem. Explor. Environ. Anal. 10, 27–74.

Hanly, A.J., 2001. The Mineralogy, Petrology and Rare Earth Element Geochemistry of the Maw Zone, Athabasca Basin, Canada, University of Missouri–Rolla, Unpublished M.Sc. thesis.

Hron, K., Templ, M., Filzmoser, P., 2010. Imputation of missing values for compositional data using classical and robust methods. Comput. Stat. Data Anal. 54, 3095–3107.

Jefferson, C.W., Thomas, D.J., Gandhi, S.S., Ramaekers, P., Delaney, G., Brisbin, D., Cutts, C., Portella, P., Olson, R.A., 2007. Unconformity-associated uranium deposits of the athabasca basin, Saskatchewan and Alberta. In: Jefferson, C.W., Delaney, G. (Eds.), EXTECH IV: Geology and Uranium Exploration TECHnology of the Proterozoic Athabasca Basin, Saskatchewan and Alberta. Geological Survey of Canada, Bulletin 588, pp. 23–68.

Jolliffe, I.T., 1986. Principal Component Analysis. Encyclopedia of Statistics in Behavioral Science. John Wiley & Sons, Ltd.

Klovan, J.E., Imbrie, J., 1971. An algorithm and fortran IV program for large-scale Q–mode factor analysis and calculation of factor scores. Math. Geol. 3, 61–67.

Knox, A. 1985. Geology and yttrium mineralization of the MAW zone, Wheeler River property, northernSaskatchewan; Union Oil Company of Canada Ltd., unpublished report, 89 pp.

MacDougall, D.G., 1990. Rare earth elementmineralization in the Athabasca Group – Mawzone. Summary of investigations. Saskatchewan geological survey, SaskatchewanEnergy and Mines, Report 90–4, pp. 103–105.

Mwenifumbo, C.J., Bernius, G.R., 2007. Crandallite-group minerals: host of thorium enrichment in the eastern athabasca basin, Saskatchewan. In: Jefferson, C.W., Delaney, G. (Eds.), EXTECH IV: Geology and Uranium Exploration TECHnology of the

Proterozoic Athabasca Basin, Saskatchewan and Alberta. Geological Survey of Canada, Bulletin 588, pp. 521–532.

Normand, C., 2014. Rare earths in Saskatchewan: mineralization types, settings, and distributions; Saskatchewan ministry of the economy. Saskatchwan Geological Survey Report 264.

O'Connell, I., Hattori, K., Chen, S., Adlakha, E., Sorba, C., 2015. Characterization of tourmaline from the Maw zone, Gryphon zone and sandstones above the Phoenix uranium deposits, Athabasca Basin, Saskatchewan, Canada. Geol. Sur. Can. Sc. Present. 37.

Pan, Y., Yeo, G., Rogers, B., Austman, C., Hu, B., 2013. Application of natural radiation-induced defects in quartz to uranium exploration: a case study on the Maw zone, Athabasca basin. J. Explor. Min. Geol. 21, 115–128.

Pearson, K., 1897. Mathematical contributions to the theory of evolution: on a form of spurious correlation which may arise when indices are used in the measurements of organs. Proceedings of the Royal Society of London. 60, pp. 489–498.

Quirt, D., Kotzer, T., Kyser, T.K., 1991. Tourmaline, phosphate minerals, zircon and pitchblende in the Athabasca group: Maw zone and McArthur River areas, in summary of investigations 1991. Saskatchewan Geological Survey, Saskatchewan Energy and Mines, Report. 91-4, pp. 181–191.

Ramaekers, P., Jefferson, C.W., Yeo, G.M., Collier, B., Long, D.G.F., Drever, G., Wheatley, K., 2007. Revised geological map and stratigraphy of the Athabasca group, Saskatchewan and Alberta. In: Jefferson, C.W., Delaney, G. (Eds.), EXTECH IV: Geology and Uranium Exploration TECHnology of the Proterozoic Athabasca Basin, Saskatchewan and Alberta. Geological Survey of Canada Bulletin 588, pp. 155–190.

R Core Team., 2013. R: A Language and Environment for Statistical Computing_. R Foundation for Statistical Computing, Vienna, Austria. (<URL: http://www.R-project.org/>).

Reimann, C., Filzmoser, P., Garrett, R., Dutter, R., 2011. Statistical Data Analysis Explained: Applied Environmental Statistics with R. John Wiley & Sons.

Roscoe, W., 2014. Technical report on a mineral resource estimate update for the Phoenix Uranium Deposit. Wheeler River Project, Eastern Athabasca Basin, Northern Saskatchewan, Canada. NI 43-101 Report (http://www.denisonmines.com/s/Home.asp).

Taylor, S.R., McLennan, S.M., 1985. The Continental Crust: Its Composition and Evolution. Blackwell Scientific Publications.

Templ, M., Hron, K., Filzmoser, P., 2010. robCompositions: robust estimation for compositional data. Manual and package, version 1.3.3. (https://cran.r-project.org/web/packages/robCompositions/index.html)

Yeo, G., Delaney, G., 2007. The Wollaston supergroup, stratigraphy and metallogeny of a Paleoproterozoic Wilson cycle in the trans-Hudson Orogen, Saskatchewan. In: Jefferson, C.W., Delaney, G. (Eds.), EXTECH IV: Geology and Uranium Exploration TECHnology of the Proterozoic Athabasca Basin, Saskatchewan and Alberta. Geological Survey of Canada. Bulletin 588, pp. 89–117.

Zhou, D., Chang, T., Davis, J.C., 1983. Dual extraction of R-mode and Q-mode factor solutions. Math. Geol. 15, 581–606.